

# High-Resolution Study of Composite Cavity Effects for p-Ge Lasers

Eric W. Nelson, Sandra H. Withers, Andrei V. Muravjov, Remco C. Strijbos, Robert E. Peale, Sergei G. Pavlov, Valery N. Shastin, and Chris J. Fredricksen

**Abstract**—The temporal dynamics, spectrum, and gain of the far-infrared p-Ge laser for composite cavities consisting of an active crystal and passive transparent elements have been studied with high temporal and spectral resolution. Results are relevant to improving the performance of mode-locked or tunable p-Ge lasers using intracavity modulators or wavelength selectors, respectively. It is shown that an interface between the active p-Ge crystal and a passive intracavity spacer causes partial frequency selection of the laser modes, characterized by a modulation of their relative intensities. Nevertheless, the longitudinal mode frequencies are determined by the entire optical length of the cavity and not by resonance frequencies of intracavity sub-components. Operation of the p-Ge laser with multiple interfaces between Ge, Si, and semi-insulating GaAs elements, or a gap, is demonstrated as a first step toward a p-Ge laser with an external quasi-optical cavity and distributed active media.

**Index Terms**—Laser modes, laser tuning, submillimeter wave lasers, submillimeter wave resonators, submillimeter wave spectroscopy, submillimeter wave technology.

## I. INTRODUCTION

THE far-infrared p-Ge laser [1], based on intersubband transitions of hot holes, has a wide homogeneous gain spectrum [2], which allows tuning over the spectral range 50–140  $\text{cm}^{-1}$  (70–200  $\mu\text{m}$  or 1.5–4.2 THz) [3]–[7] or generation of picosecond pulses of far-infrared radiation [8]–[14]. The traditional electrodynamic cavity of a p-Ge laser consists of a bulk p-Ge rod with external mirrors attached to its ends. Such a laser operates on a wide spectrum of active intersubband transitions and normally generates microsecond pulses of far-infrared radiation in a broad spectrum, which consists of many longitudinal modes. To generate spectrally pure single-mode emission or ultrashort pulses, the laser design may require composite cavities that include passive intracavity optical elements [3]–[7], [14]. Examples include transparent, electrically isolating silicon spacers, which have been used as part of tunable intra-

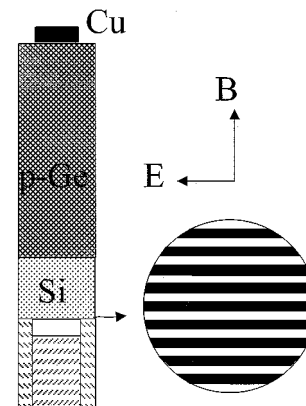


Fig. 1. Schematic of p-Ge laser cavity used for wavelength selection.

cavity wavelength selectors (Fig. 1) [3]–[7] and intracavity electrooptic modulators or passive saturable intracavity absorbers [14], which might be used for active or passive mode locking, respectively. However, use of passive intracavity optical elements in p-Ge laser cavities can introduce undesirable effects because of intrinsic reflections and loss at interfaces between optical components. Intracavity spacers of Si or pure Ge have been used by a number of authors [1], but clear understanding of the effect of losses and reflections by intracavity interfaces on p-Ge laser spectrum and emission dynamics was missing.

In this paper, data are presented that demonstrate potential problems with p-Ge laser operation and tunability, which might appear because of the presence of passive spacers in the laser cavity. The detailed experimental measurements were performed both in the spectral and time domains. Spectra were measured at high resolution ( $0.025 \text{ cm}^{-1}$ ) sufficient to resolve individual longitudinal modes for the laser cavity used. Single-shot transient recordings of the laser emission were collected at a temporal resolution ( $<100 \text{ ps}$ ), which is much faster than the cavity round-trip time. Also, the effect on gain of passive intracavity elements was studied qualitatively in terms of threshold electric and magnetic fields.

Silicon, pure Ge, and GaAs were chosen as cavity inserts because all have low absorption at p-Ge laser emission wavelengths and active p-Ge has relatively low small-signal gain [15]. Also, the refractive index of these materials is sufficiently close to that of Ge in that only  $\sim 1\%$  reflection is expected at each interface when the interface is of optical quality. The operation of a p-Ge laser with a liquid-helium filled gap between active crystal and back mirror was demonstrated in anticipation of future open-cavity configurations.

Manuscript received May 2, 2001; revised August 20, 2001. The work of S. G. Pavlov and V. N. Shastin was supported in part by INTAS under Grant 97-0856. This work was supported by the National Science Foundation under an AFOSR STTR Phase I Award.

E. W. Nelson, S. H. Withers, A. V. Muravjov, and R. E. Peale are with the Department of Physics, University of Central Florida, Orlando, FL 32816 USA (e-mail: rep@physics.ucf.edu).

R. C. Strijbos is with JDS Uniphase, Eindhoven, The Netherlands.

S. G. Pavlov and V. N. Shastin are with the Institute for Physics of Microstructures, Russian Academy of Sciences, GSP-105, Nizhny Novgorod 603600, Russia.

C. J. Fredricksen is with Zauberte Inc., Orlando, FL 32826 USA.

Publisher Item Identifier S 0018-9197(01)10252-6.

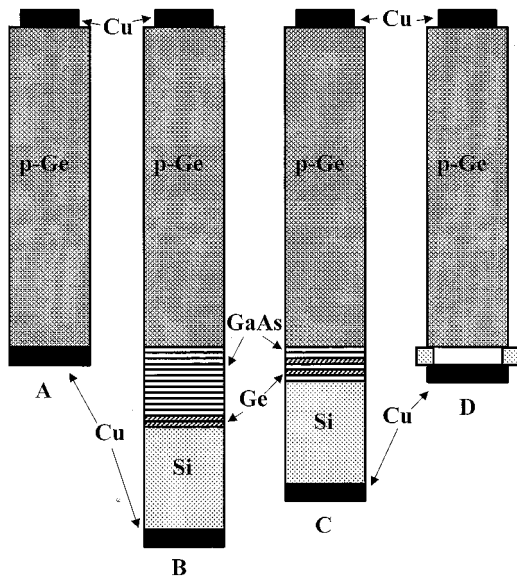


Fig. 2. Experimental cavity constructions. In each case, additional elements were sandwiched between a 27.975-mm active p-Ga crystal and a 7-mm Cu back mirror. The constructions were: (a) 25- $\mu$ m teflon/active p-Ge/25- $\mu$ m teflon; (b) teflon/active p-Ge/12 0.5-mm GaAs plates/two 0.5-mm intrinsic Ge plates/9-mm Si spacer; (c) teflon/active p-Ge/two GaAs plates/Ge plate/GaAs plate/Ge plate/GaAs plate/Si spacer; and (d) teflon/27.975-mm crystal/gap provided by a Si ring.

## II. EXPERIMENT

Laser crystals were cut from monocrystalline Ge doped by Ga with  $N_A \approx 7 \times 10^{13} \text{ cm}^{-3}$  in the form of a rectangular parallelepiped  $5 \times 7 \times L \text{ mm}^3$  ( $L_1 = 27.975 \pm 0.005 \text{ mm}$  and  $L_2 = 50.240 \pm 0.005 \text{ mm}$ ) with the long axis along the [110] crystallographic axis. Electric field pulses of 1–2- $\mu$ s duration were applied along the  $[-110]$  axis via ohmic contacts evaporated on opposite lateral sides. The crystal end faces were polished parallel to each other within 1 arc minute accuracy. The surface roughness in the central portion of the active crystal ends was determined to be  $\sim 10 \text{ nm}$ . The edges were unintentionally rounded during polishing, giving a final deviation from flatness of 100 nm. The basic laser cavity was formed by two copper mirrors attached to the sample end faces via 20  $\mu$ m of isolating teflon film (Fig. 2). The output mirror had a diameter of 4 mm, which was smaller than the active sample cross section to allow some radiation to escape around the mirror edge. The system was cooled by liquid helium and immersed in an external magnetic field created by a superconducting solenoid in Faraday configuration ( $B \parallel [110]$ ), or by a room temperature external electromagnet in Voigt configuration ( $B \parallel [001]$ ). The strengths of the applied electric and magnetic fields could be independently varied to determine the  $E$  and  $B$  lasing thresholds.

The laser beam propagated along the long crystal axis [110] was conducted out of the cryostat using a brass light pipe and was detected after a teflon lens with a fast whisker-contacted Schottky diode.<sup>1</sup> The signal was amplified<sup>2</sup> and recorded on a transient digitizer<sup>3</sup> with 4.5-GHz analog bandwidth, oversampled at 200 Gs/s. For spectral measurements, the radiation was

<sup>1</sup>IT17(82), University of Virginia.

<sup>2</sup>Picosecond Pulse Labs 5840, 10-GHz bandwidth.

<sup>3</sup>Tektronix SCD5000.

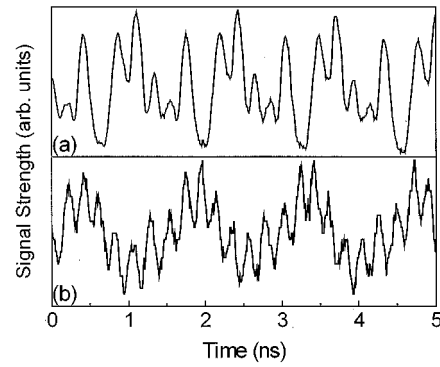


Fig. 3. Transient recording of 50.240-mm p-Ge crystal laser emission: (a) without and (b) with a Si spacer in the cavity.

directed to a Bomem DA8 Fourier spectrometer with an unapodized instrumental line width of  $0.025 \text{ cm}^{-1}$ , equipped with an event-locking accessory (Zaubertek) for low duty sources [16]. The modulated signal was detected by a liquid-helium cooled Si composite bolometer.

The laser operation was tested using cavities that contained spacers made of Si, pure Ge, semi-insulated GaAs, and also a liquid-helium filled gap between the laser crystal and back mirror [Fig. 2(b)–(d)]. Si spacers were cut to a length of  $\sim 8 \text{ mm}$  from monocrystalline Si and had the same flatness and parallelism of the surfaces as p-Ge samples. The GaAs was standard semi-insulating substrate material cut from 0.5-mm wafers purchased from the M.T.I. Corporation. These double-side polished commercial wafers had a 3 arc minute wedge, which was compensated by using pieces in pairs, cut from neighboring regions of the wafer, with one of the pieces rotated  $180^\circ$  about the plane normal. The pure Ge sample (approximately  $7 \times 14 \text{ mm}^2$ ) was cut from a single-side polished 0.5-mm wafer from Atramet. The rough side was hand polished using a low-speed glass wheel with a nylon pad and Buehler 1  $\mu$ m diamond suspension in water as the final step. After that, the sample piece was cut in half and the residual wedge compensated as for the GaAs.

The cavity construction shown in Fig. 2(d) had a Si ring with an inner diameter of 6 mm, an outer diameter of 9 mm, and 1.5-mm thickness, inserted between the active crystal and the back mirror. The purpose of the ring was to create a gap while keeping the back mirror parallel to the active crystal face.

## III. RESULTS

The periodic temporal structure of the single laser shot from the 50.240-mm crystal with mirrors [Fig. 2(a)] is shown in Fig. 3(a). The period of main oscillations equals the calculated roundtrip time  $\tau_{Ge} = 2n_{Ge}L_{Ge}/c = 1316 \pm 0.8 \text{ ps}$  ( $n_{Ge} = 3.925 \pm 0.002$  [17]). The same structure with an  $8.375 \pm 0.005$ -mm-long polished Si spacer ( $n_{Si} = 3.384 \pm 0.002$  [17]), installed between the Ge crystal and back mirror, reveals a high-frequency component superimposed onto lower frequency oscillations. The observed period of fast oscillations is  $\tau_{fo} = 215 \text{ ps}$ .

The average of a series of Fourier transforms of data such as in Fig. 3(a) and (b) are presented in Fig. 4(a) and (b). For the laser cavity with the 50.240-mm crystal without an

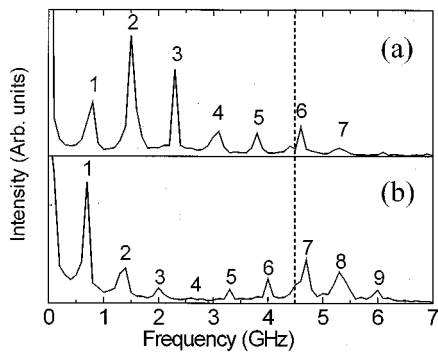


Fig. 4. Fourier transform of transient records for 50.240 mm p-Ge laser emission: (a) without and (b) with a Si spacer in the cavity. Dashed line: the 4.5-GHz instrumental bandwidth.

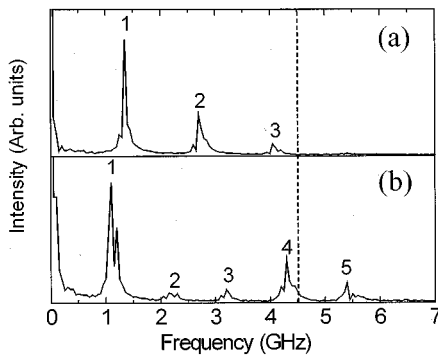


Fig. 5. Fourier transform of transient records for 27.975 mm p-Ge laser emission: (a) without and (b) with a Si spacer in the cavity ( $E = 1.43$  kV/cm,  $B = 0.92$  T for both cases). Dashed line: the 4.5-GHz instrumental bandwidth.

insert [Fig. 4(a)], harmonics (numbered) of the fundamental round-trip frequency 760.0 MHz (“1”) are observed up to the seventh. Harmonics 5 and up are attenuated by the 4.5-GHz bandwidth of the electronics. For the same laser with the Si spacer [Fig. 4(b)], harmonics up to the ninth are observed and their spacing is smaller than in Fig. 4(a), owing to the smaller round-trip frequency  $664.5 \pm 0.5$  MHz for the combined cavity. Compared to Fig. 4(a), the second and third harmonics are strongly suppressed and the higher harmonics are relatively more pronounced.

Fig. 5 shows similar results for the 27.975-mm crystal. Without a Si spacer, three harmonics of the 1.365-GHz fundamental are observed [Fig. 5(a)]. With a Si spacer, fast oscillations are again observed with a period  $\tau_{fo} = 230$  ps. Harmonics of the combined cavity’s  $1.085 \pm 0.001$ -GHz fundamental can be seen [Fig. 5(b)] up to the fifth, where the fourth and fifth have grown at the expense of the second. The periods and frequencies of the prominent oscillations noted so far are summarized in Table I for both long and short active crystals.

Fig. 6 shows a spectrum of the p-Ge laser with tunable frequency selector (see Fig. 1). The cavity consisted of the 27.975-mm active crystal with a  $7.865 \pm 0.005$  mm long Si spacer, giving  $\tau_{Si}$  of  $177.6 \pm 0.2$  ps and  $\tau_c$  of  $910.1 \pm 0.7$  ps for this construction. A lamellar-type wavelength selector with a gap  $\sim 140$   $\mu\text{m}$  [3]–[6] was included in this cavity (Fig. 1). Recently, it was discovered that the selection efficiency (active cavity finesse) strongly depends on the precise position of

the tunable mirror [6]. For Fig. 6, a spectrum was chosen for which the laser failed to operate in a single frequency mode, generating multiple modes instead, for the purpose of investigating the causes of such behavior. Four modes with peaks at  $106.06$ ,  $106.24$ ,  $106.42$ , and  $106.60 \pm 0.02$   $\text{cm}^{-1}$  are apparent, for a spacing of  $0.18 \pm 0.02$   $\text{cm}^{-1}$ . This separation is nearly five times the axial mode spacing  $0.0366$   $\text{cm}^{-1}$  of the entire cavity. No other peaks appear in the range  $40$ – $140$   $\text{cm}^{-1}$ .

Fig. 7 presents the observed  $E \times B$  generation zones for the four cavity constructions shown in Fig. 2.

#### IV. DISCUSSION

The laser intensity seen in Fig. 3 is clearly periodic, with a period equal to the round-trip cavity time. In addition, there is a finer pattern of mode interference within one period that depends on the initial random-phase distribution of the modes, which differs for each laser shot. The calculated round-trip times of the full cavities (active Ge crystal with Si spacer)  $\tau_c = (2/c)(n_{Ge}L_{Ge} + n_{Si}L_{Si})$  are given for each setup in Table I. The optical thickness of the teflon film on the mirror and the phase shift on the boundaries were neglected in calculations of round-trip times because the optical length of the active Ge crystal and Si spacer is  $10^3$  to  $10^4$  times larger than the teflon film thickness and the radiation wavelength. The time of propagation of the radiation inside the teflon film less than 0.2 ps, which is less than the uncertainty in  $\tau_c$ . The calculated round-trip time  $\tau_{Si} = 2n_{Si}L_{Si}/c$  for internal reflections within the 8.375-mm Si spacer is also given in Table I. The observed fast oscillation periods  $\tau_{fo}$  in Fig. 3(b) is (within experimental uncertainty) an exact harmonic of  $\tau_c$ , i.e.,  $\tau_{fo} = \tau_c/q$ , where  $q$  is 7 for the cavity consisting of a 50.240-mm Ge crystal and a Si spacer and  $q$  is 4 for the 27.975-mm crystal and Si spacer. In each case,  $\tau_{fo}$  differs significantly from  $\tau_{Si}$ . This confirms that the development of the p-Ge laser radiation occurs at longitudinal mode frequencies of the full laser cavity defined by the end mirrors. Within the accuracy of the data presented here, reflections and scattering of the laser radiation on intracavity interfaces do not affect the laser mode spacing. Rather, the only observed effect of an interfaces is modulation of the relative mode intensities, as well be shown below.

Harmonics of the fundamental round-trip frequency occur in Figs. 4 and 5 because of beating between different pairs among the ensemble of evenly spaced [14] axial modes. These modes are defined by frequencies  $f_p = p/\tau_c$ , where the mode index  $p$  is an integer. The redistribution of energy in the frequency spectrum of mode beating caused by the insertion of the optical spacer [Figs. 4(b) and 5(b)] can be explained in terms of losses and scattering at the Si/Ge interface and competition between modes in the active Ge crystal. Small loss modes will be more prominent in the laser output. Losses, which can occur from interface absorption or scattering, are expected to be largest for those modes having a large amplitude of the oscillating electric field at the interface and smallest for modes with interface nodes, as shown schematically in Fig. 8. Small loss modes are, therefore,  $f_q = q/\tau_{Si}$ , where  $q$  is as close as possible to an integer. Thus, for the 50.240-mm sample, minimum-loss combined cavity modes occur when  $f_p = f_q$  or  $p = (\tau_c/\tau_{Si})q =$

TABLE I  
SUMMARY OF ROUND-TRIP TIMES FOR CONSTRUCTIONS USED IN MEASURING EMISSION DYNAMICS.  
CORRESPONDING FREQUENCIES ARE GIVEN TO THE IMMEDIATE RIGHT OF EACH TEMPORAL VALUE

|                    |                                  | 50.240 mm crystal  |                     | 27.975 mm crystal  |                     |
|--------------------|----------------------------------|--------------------|---------------------|--------------------|---------------------|
| $\tau_{\text{Ge}}$ | round trip time in Ge crystal    | $1316 \pm 0.8$ ps  | $760.1 \pm 0.5$ MHz | $732.5 \pm 0.5$ ps | $1365 \pm 1$ MHz    |
| $\tau_c$           | round trip time in Ge + Si       | $1505 \pm 1.0$ ps  | $664.5 \pm 0.5$ MHz | $921.5 \pm 0.7$ ps | $1085 \pm 1$ MHz    |
| $\tau_{\text{fo}}$ | observed fast oscillation period | $215 \pm 5.5$ ps   | $4.65 \pm 0.12$ GHz | $230 \pm 8.0$ ps   | $4.34 \pm 0.15$ GHz |
| $\tau_{\text{Si}}$ | round trip time in Si spacer     | $189.1 \pm 0.2$ ps | $5290 \pm 6$ MHz    | $189.1 \pm 0.2$ ps | $5290 \pm 6$ MHz    |

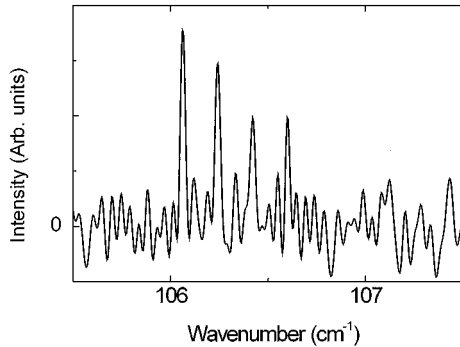


Fig. 6. Emission spectrum of p-Ge laser with intracavity wavelength selector.

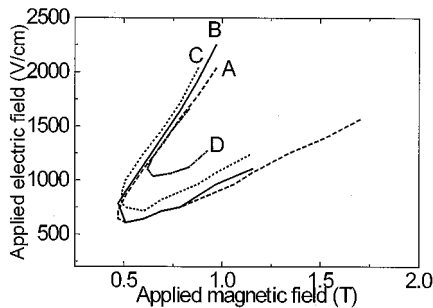


Fig. 7. Laser generation zones for four cavity constructions with different passive intracavity elements, corresponding to Fig. 2.

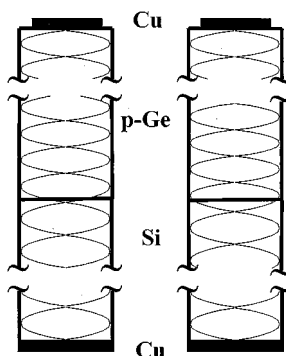


Fig. 8. Composite Si/Ge cavity showing low- and high-loss modes (left and right, respectively). Modes with nodes at the Si/Ge interface will experience the smallest loss.

$7.96 \pm 0.01q$ . The requirement for low loss that  $q$  be nearly integral means that periods  $\tau_c/8$  should be prominent in transient recordings of the composite laser and the eighth harmonic of the fundamental round-trip frequency should be the strongest in the Fourier transform of such data. Similar analysis for the 27.975-mm crystal argues that the fifth harmonic should be most prominent. The experimental fact that the seventh and the fourth

harmonics appear strongest in Figs. 4(b) and 5(b), respectively, is explained by the  $\sim 5$ -GHz instrumental bandwidth limitations.

This discussion is clarified by a simple model. The intensity of a given mode with wave vector  $k_1$  after  $m$  passes through the composite Si/Ge cavity in a linear regime of laser emission development is

$$I_m = I_0 [e^{\alpha L} - \delta \cos^2(k_1 L)]^m \quad (1)$$

where  $L$  is the active Ge crystal length and  $\alpha$  is the gain coefficient. Scattering or absorption at the Si/Ge interface with loss coefficient  $\delta$  is assumed to be proportional to the squared amplitude of the oscillating electric field of certain modes ( $k_1$ ) at the interface. The wavenumber  $k_1$  in the Ge crystal for modes having allowed frequencies for the combined cavity is  $k_1 = 2\pi n_{\text{Ge}} p / c\tau_c$ . The time dependence caused by beating between a pair of modes with mode indices  $p$  and  $p+r$ , where  $p$  and  $r$  are integers, is given by

$$|E(p, r)|^2 \approx I_m(p) + I_m(p+r) + 2[I_m(p)I_m(p+r)]^{1/2} \cdot \cos\left(\frac{2\pi r t}{\tau_c}\right). \quad (2)$$

The third term represents beat oscillations with frequencies  $r/\tau_c$ , which cannot be observed with our detection electronics not beyond about 5–6 GHz. For a given  $r$ , the amplitude of the beat oscillation depends on the mode number  $p$ . Since hundreds of modes can oscillate simultaneously, the spectrum of observable beats  $y(r)$  is found by averaging (summing) the amplitude over many  $p$  values

$$y(r) = \sum_{p=3000}^{p=4000} [I_m(p)I_m(p+r)]^{1/2}. \quad (3)$$

Fig. 9 shows the calculated beat spectrum, according to (3) for the Si plus 50.240-mm Ge cavity, as the white bars. Parameters used were  $\delta = 0.007$ ,  $\alpha = 0.028 \text{ cm}^{-1}$  and  $m \approx 1300$ . The gain value of  $\alpha$  corresponds to a typical experimental value [15]. The number of passes ( $m \approx 1300$ ) is a realistic value for a characteristic  $1 \mu\text{s}$  emission pulse duration. The minimum and maximum  $p$  values correspond to minimum ( $70 \text{ cm}^{-1}$ ) and maximum ( $90 \text{ cm}^{-1}$ ) frequencies when fields of approximately  $B = 0.9 \text{ T}$  and  $E = 1.4 \text{ kV/cm}$  are applied to a cavity consisting of the 50.240 mm Ge crystals with the 8.375-mm Si spacer. The dashed line is a possible power attenuation function, which is the product of a first order filter with a 4.5-GHz cutoff (modeling the SCD 5000 transient digitizer) and a second filter term modeling all other components in the detection circuit. The solid bars plot the product of the calculated beat spectrum with the frequency attenuation function. A loss coefficient  $\delta$  of 0.007 gave a beat

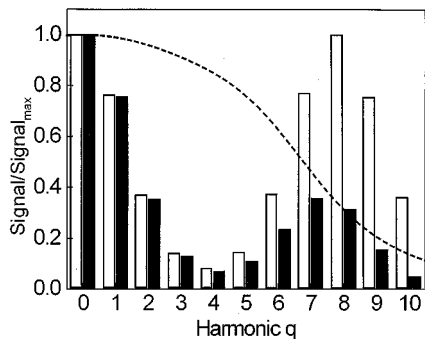


Fig. 9. Modeled beat spectrum for the p-Ge laser with Si intracavity spacer. Modeled roll-off for detection electronics is shown by the dashed line.

TABLE II  
 $p$  AND  $q$  VALUES FOR OBSERVED SPECTRAL PEAKS. THE ESTIMATED UNCERTAINTIES ON CENTER FREQUENCY,  $p$ , AND  $q$  VALUES ARE  $0.02 \text{ cm}^{-1}$ , 3, AND 2, RESPECTIVELY

| Observed Frequency Peak ( $\text{cm}^{-1}$ ) | 106.06 | 106.24 | 106.42 | 106.60 |
|--|--------|--------|--------|--------|
| Calculated $p$ -value                        | 2894   | 2899   | 2904   | 2909   |
| Calculated $q$ -value                        | 565.   | 566.   | 567.   | 568.   |

spectrum (Fig. 9, solid bars) in qualitative agreement with the data of Fig. 4(b). The seventh harmonic of the fundamental frequency is most prominent and the fourth harmonic is strongly suppressed.

This interpretation of temporal observations is supported by the spectroscopic measurements (Fig. 6), which permit an estimate of the mode index  $p$  for each of the four laser lines observed. The integral values of  $p$ , given in Table II, were calculated based on the 910.1-ps round-trip time  $\tau_c$ . As before, the  $p$  and  $q$  values for strong modes are related by  $p = (\tau_c/\tau_{\text{Si}})q$ , with  $q$  being nearly an integer. The difference in  $p$  values for neighboring prominent modes is five, in agreement with the ratio  $(\tau_c/\tau_{\text{Si}}) = 5.12 \pm 0.01$  for this cavity. The error margins are introduced mainly by uncertainty in the indices of refraction.

Fig. 7 shows regions of the laser operation in the plane of  $E$  and  $B$  applied field strengths for different tested cavity constructions. The width of these regions is an indirect indication of the value of the averaged gain in the full system. The results show that lasing is not significantly affected by the number of intracavity interfaces, by the number of interfaces with a change in index, or by substantial passive thicknesses of Si, GaAs, or pure Ge. The data indicate, however, that introducing a vacuum gap into the cavity may introduce loss. This could be caused by increased reflections at the vacuum/p-Ge interface due to the rather large disparity of the indices of refraction.

## V. CONCLUSION

The combined cavity effects reported here are important for the development of a tunable p-Ge laser system, mode-locking with intracavity modulators, and open quasioptical cavities. Tunable intracavity frequency selectors used by all investigators to date [3]–[7] have incorporated a silicon or pure germanium spacer in their design. Although such selectors are capable of selecting a single longitudinal mode at certain frequencies [5],

they experience difficulties with fine continuous tunability [6]. These problems are due to preferred amplification of those longitudinal modes which fall close to spacer resonances.

An alternative method of tuning a p-Ge laser is based on cyclotron resonance transitions of light holes. This is achieved without intracavity elements and is free from the related tuning problems mentioned above. However, this mode of operation requires large tunable magnetic fields that can only be provided by liquid-helium-cooled superconducting solenoids. The linewidth of the cyclotron resonance emission is  $\sim 0.2 \text{ cm}^{-1}$  [18], which contains a number of longitudinal modes. The output is generally weaker by 1–2 orders of magnitude than that for the p-Ge intersubband laser mechanism. In contrast, the intersubband p-Ge laser with a tunable intracavity frequency selector can generate emission of a single longitudinal mode [5], which has megahertz line width. Moreover, such tuning elements can be electrically controlled [6], and this mode of operation allows the use of uncooled permanent magnet assemblies [19].

The interface problems for tunable selectors discussed in this paper could be solved, in principle, by improving the quality of contacting surfaces, although great care has already been expended in our experiments to make all surfaces flat, clean, and highly polished. Another possibility is to wedge the interface. However, it seems ultimately more practical to entirely eliminate passive transparent spacers, whose purpose is primarily electrical isolation of metal parts from high-voltage contacts. This could be done, for example, by using the dielectric  $\text{SrTiO}_3$  as high-reflectivity tuner mirrors instead of brass or copper.

For mode-locked p-Ge lasers, there has been only one report of the use of an intracavity element, which was found to strengthen a self-modelocking effect [14]. Use of intracavity modulators or saturable absorbers is very attractive compared with current art, in which high-power electrical gain modulation is applied directly to the active crystal via extra contacts. Spacer resonance effects, such as those described here, should be avoided to prevent distortion of generated pulses.

Another feature demonstrated in this paper is the operation of a p-Ge laser with multiple intracavity spacers, which is a step toward distributing the active media as a thermal management scheme. The spacers studied here, namely Si, GaAs and pure Ge, all have high thermal conductivity and high far-infrared transparency.

Finally, p-Ge laser operation has been demonstrated for a cavity which has a liquid-helium-filled gap between an external laser mirror and the active crystal. This offers promise for the development of continuously tunable p-Ge lasers with changeable cavity length, which is required for continuous tuning without mode hops. The cavity mirror might be moved entirely outside the cryostat to facilitate adjustments, experimentation, and applications. As a step in this direction, we recently demonstrated a p-Ge laser with an open semiconfocal resonator, which will be the subject of a forthcoming paper.

## REFERENCES

- [1] E. Gornik and A. A. Andronov, Eds., *Opt. Quantum Electron.*, London, U.K.: Chapman and Hall, 1991, vol. 23.
- [2] F. Keilmann and R. Till, "Saturation spectroscopy of the p-Ge far-infrared laser," *Opt. Quantum Electron.*, vol. 23, pp. S231–S246, 1991.

- [3] S. Komiyama, H. Morita, and I. Hosako, "Continuous wavelength tuning of inter-valence-band laser oscillation in p-type germanium over range of 80–120  $\mu\text{m}$ ," *Jpn. J. Appl. Phys.*, pt. 1, vol. 32, pp. 4987–4991, 1993.
- [4] A. V. Murav'ev, I. M. Nefedov, S. G. Pavlov, and V. N. Shastin, "Tunable narrowband laser that operates on interband transitions of hot holes in germanium," *J. Soviet Quantum Electron.*, vol. 23, pp. 119–124, 1993.
- [5] A. V. Muravjov, S. H. Withers, H. Weidner, R. C. Strijbos, S. G. Pavlov, V. N. Shastin, and R. E. Peale, "Single axial-mode selection in a far-infrared p-Ge laser," *Appl. Phys. Lett.*, vol. 76, pp. 1996–1998, 2000.
- [6] E. W. Nelson, A. V. Muravjov, S. G. Pavlov, V. N. Shastin, and R. E. Peale, "Piezo controlled intracavity wavelength selector for the far-infrared p-Ge laser," *Infrared Phys. Tech.*, vol. 42, pp. 107–110, 2001.
- [7] P. W. Smith, "Mode selection in lasers," *Proc. IEEE*, vol. 60, pp. 422–440, 1972.
- [8] R. C. Strijbos, J. G. S. Lok, and W. T. Wenckebach, "A Monte Carlo simulation of mode-locked hot-hole laser operation," *J. Phys. Condens. Matter*, vol. 6, pp. 7461–7468, 1994.
- [9] J. N. Hovenier, A. V. Muravjov, S. G. Pavlov, V. N. Shastin, R. C. Strijbos, and W. T. Wenckebach, "Active mode locking of a p-Ge hot hole laser," *Appl. Phys. Lett.*, vol. 71, pp. 443–445, 1997.
- [10] A. V. Muravjov, R. C. Strijbos, C. J. Fredricksen, H. Weidner, W. Trimble, A. Jamison, S. G. Pavlov, N. Shastin, and R. E. Peale, "Mode-locked far-infrared p-Ge laser using an offset rf electric field for gain modulation," in *Tech. Dig. Workshop on Radiative Processes and Dephasing in Semiconductors*, vol. 18, D. Citron, Ed., Washington, DC, 1998, pp. 102–107.
- [11] J. N. Hovenier, T. O. Klaassen, W. Th. Wenckebach, A. V. Muravjov, S. G. Pavlov, and V. N. Shastin, "Gain of the mode locked p-Ge laser in the low field region," *Appl. Phys. Lett.*, vol. 72, pp. 1140–1142, 1998.
- [12] A. V. Muravjov, R. C. Strijbos, C. J. Fredricksen, S. H. Withers, W. Trimble, S. G. Pavlov, V. N. Shastin, and R. E. Peale, "Pulse separation control for mode-locked far-infrared p-Ge lasers," *Appl. Phys. Lett.*, vol. 74, pp. 167–169, 1999.
- [13] A. V. Muravjov, S. H. Withers, R. C. Strijbos, S. G. Pavlov, V. N. Shastin, S. G. Pavlov, and R. E. Peale, "Actively mode-locked p-Ge laser in Faraday configuration," *Appl. Phys. Lett.*, vol. 75, pp. 2882–2884, 1999.
- [14] A. V. Muravjov, R. C. Strijbos, C. J. Fredricksen, H. Weidner, W. Trimble, S. H. Withers, S. G. Pavlov, V. N. Shastin, and R. E. Peale, "Evidence for self-mode-locking in p-Ge laser emission," *Appl. Phys. Lett.*, vol. 73, pp. 3037–3039, 1998.
- [15] A. V. Muravjov, S. H. Withers, S. G. Pavlov, V. N. Shastin, and R. E. Peale, "Broad band p-Ge optical amplifier of terahertz radiation," *J. Appl. Phys.*, vol. 86, pp. 3512–3515, 1999.
- [16] H. Weidner and R. E. Peale, "Event-locked time-resolved Fourier spectroscopy," *Appl. Spectros.*, vol. 51, pp. 1106–1112, 1997.
- [17] E. V. Loewenstein, D. R. Smith, and R. L. Morgan, "Optical constants of far infrared materials 2: Crystalline solids," *Appl. Opt.*, vol. 12, pp. 398–406, 1973.
- [18] E. Gornik, K. Unterrainer, and C. Kremser, "Tunable far-infrared solid-state lasers based on hot holes in germanium," in *Opt. Quantum Electron.*, 1991, vol. 23, pp. S267–S286.
- [19] Kijun Park, R. E. Peale, H. Weidner, and J. J. Kim, "Submillimeter p-Ge laser using a voigt-configured permanent magnet," *IEEE J. Quantum Electron.*, vol. 32, pp. 1203–1210, 1996.

**Eric W. Nelson** received the B.S. degree in engineering physics from the University of West Florida, Pensacola, in 1997, and the M.S. degree in optics in 2000 from the University of Central Florida (UCF), Orlando, where he is currently working toward the Ph.D. degree in physics, studying p-Ge lasers.

**Sandra H. Withers** received the B.S. and M.S. degrees in physics in 1997 and 2000, both from the University of Central Florida (UCF), Orlando, where she is currently working toward the Ph.D. degree, studying metal ion impurities in geologic minerals.

**Andrei V. Muravjov** received the B.A. degree in physics and the M.S. degree in radiophysics and electronics in 1982 and 1984, respectively, from the Gorky State University, Nizhny Novgorod, Russia, and the Ph.D. degree in physics and mathematics in 1992 from the Institute of Applied Physics, Russian Academy of Science, Nizhny Novgorod.

He currently holds the position of Senior Researcher at Institute for Physics of Microstructures, Russian Academy of Science, and is also a Research Associate at the University of Central Florida, Gainesville. He has traveled widely as a visiting scholar assisting p-Ge laser development efforts in Germany, Holland, and the U.S.

**Remco C. Strijbos** received the Ph.D. degree in physics from Delft University of Technology, The Netherlands, in 1997.

Subsequently, he held a post-doctoral position at the University of Central Florida, Orlando. He investigated hot hole transport in p-Ge in relation to active mode-locking of far-infrared p-Ge lasers by gain modulation. In 1999, he moved to the Eindhoven University of Technology, The Netherlands, to work on polarization control of intra-cavity contacted VCSELs. He is now a Research Scientist at JDS Uniphase, Eindhoven, The Netherlands.

**Robert E. Peale** received the B.A. degree in physics from the University of California at Berkeley in 1983, the M.S. degree in physics in 1986 and the Ph.D. degree in physics in 1990, both from Cornell University, Ithaca, NY.

He held a post-doctoral position at Lehigh University, Bethlehem, PA, and has been on the faculty at the University of Central Florida, Orlando, since 1991. His research activities include spectroscopic studies of impurities in ionic and semiconducting crystals, optical engineering in support of operations at the Kennedy Space Center, instrumentation development, and far-infrared p-Ge lasers.

**Sergei G. Pavlov** is a Researcher at the Institute for Physics of Microstructures, Russian Academy of Science, Nizhny Novgorod. He is currently a Humboldt Fellow at the Institute for Space Sensor Technology, Berlin, Germany.

**Valery N. Shastin** is the Head of the Laboratory for Far Infrared Lasers at the Institute for Physics of Microstructures, Russian Academy of Science, Nizhny Novgorod.

**Chris J. Fredricksen** received the B.S. and M.S. degrees in physics in 1996 and 1998, respectively, from the University of Central Florida, Orlando.

He was Principal Investigator on an Air Force funded p-Ge laser STTR Phase I Award to Zaubertek.